

Eastward expansion of the Tibetan Plateau by crustal flow and strain partitioning across faults

Qi Yuan Liu^{1*}, Robert D. van der Hilst², Yu Li¹, Hua Jian Yao³, Jiu Hui Chen¹, Biao Guo¹, Shao Hua Qi¹, Jun Wang¹, Hui Huang² and Shun Cheng Li¹

The lateral expansion of the southeastern Tibetan Plateau causes devastating earthquakes, but is poorly understood. In particular, the links between regional variations in surface motion^{1–3} and the deeper structure of the plateau are unclear. The plateau may deform either by movement of rigid crustal blocks along large strike-slip faults^{4,5}, by continuous deformation^{6,7}, or by the eastward flow of a channel of viscous crustal rocks^{8,9}. However, the importance of crustal channel flow was questioned in the wake of the 2008 Wenchuan earthquake^{10–12}. Controversies about the style of deformation have persisted, in part because geophysical probes have insufficient resolution to link structures in the deep crust to the observed surface deformation. Here we use seismic data recorded with an array of about 300 seismographs in western Sichuan, China, to image the structure of the eastern Tibetan Plateau with unprecedented clarity. We identify zones of weak rocks in the deep crust that thicken eastwards towards the Yangtze Craton, which we interpret as crustal flow channels. We also identify stark contrasts in the structure and rheology of the crust across large faults. Combined with geodetic data, the inferred crustal heterogeneity indicates that plateau expansion is accommodated by a combination of local crustal flow and strain partitioning across deep faults. We conclude that rigid block motion and crustal flow are therefore not irreconcilable modes of crustal deformation.

The magnificence of the Tibetan plateau and controversies about its origin and deformation style following the collision of India and Asia some 50 Myr ago have inspired many geological and geophysical studies of Tibet and surrounding regions. Southeastern Tibet—where interaction of distinct tectonic units produces one of the most seismically active regions of China (Fig. 1)—has been central in this debate. Crustal channel flow^{8,9} was proposed to explain the conundrum of, on the one hand, the slow lateral deformation and the absence of substantial Neogene shortening structures just west of Sichuan Basin and, on the other hand, high elevation and steep relief across the Longmenshan. Zones of high electrical conductivity¹³ and low shear wave speed^{14–16} as well as depth variations of seismic anisotropy^{17,18} support this model, but its validity has been questioned, for instance, in the wake of the 2008 Wenchuan earthquake^{10–12}. The mechanisms for uplift and plateau expansion have remained enigmatic, in part, as a result of uncertainty associated with extrapolation from two-dimensional (2D) profiles, non-unique interpretation of separate data sets, and insufficient spatial resolution to relate deep structures imaged seismologically to geological observables at the surface.

Indeed, understanding eastern Tibetan plateau dynamics requires seismological constraints on 3D crustal structure at a higher spatial resolution (and over larger areas and depth ranges) than has so far been available. We can now produce this insight using data from a pioneering regional array of ~300 densely spaced seismograph stations in southeastern Tibet (Fig. 1).

Figure 1a shows the main geological, topographical, and seismotectonic features of the area defined by the interaction of geological units (Songpan, Kangding, Dianzhong, Sichuan Basin) that have distinct crustal structures, are internally deformed, and are bounded on the crustal scale by faults (Xianshuihe, Longmenshan, Lijiang, Anninghe–Zemuhe–Xiaojiang) along which most of the region's large earthquakes occur. The rate of eastward crustal movement away from central Tibet is partitioned across the Xianshuihe and Anninghe–Zemuhe–Xiaojiang faults. To the south, in Kangding and Dianzhong, which constitute the so-called Chuandian fragment, fast horizontal motions (reaching ~17 mm yr⁻¹) define the conspicuous clockwise rotation of Tibetan crust around the Eastern Himalayan Syntaxis (EHS; refs 1–4). To the north, in what we call Songpan, surface displacement is slow and decreasing eastwards, with crustal shortening near the Longmenshan fault less than 3 mm yr⁻¹ (refs 1,3).

Figure 1b shows the location of a temporary, dense (10–30 km spacing) array of almost 300 broadband seismographs in western Sichuan. From waveforms recorded between 2007 and 2009 we infer 3D variations in shear wave speed in the crust and upper mantle through joint (nonlinear) inversion of P-receiver functions and the (Rayleigh) surface-wave phase velocity dispersion from ambient noise correlation (Methods). Our 3D model agrees with seismic refraction¹⁹ profiles (Supplementary Fig. 12), but provides high-resolution insight across a large area and avoids uncertainties associated with interpolation between 2D sections.

Figure 2 illustrates 3D crustal heterogeneity through a series of map views. At shallow depth (Fig. 2a) the dense array data reveal seismically slow sediments in Sichuan Basin, fast wave propagation in Kangding, and variable but near-average wave speeds in Songpan, Dianzhong and Yangtze. In the upper crust (Fig. 2b) low wave speeds appear along the Xianshuihe fault and in the Yidun (or Shangrila) part of Kanding (west of the Litang fault), and high wave speeds correlate with parts of the Emeishan large igneous province²⁰. The most conspicuous mid-crustal features (Fig. 2c) are the anomalously low wave speeds in the Kangding unit (protruding across the Lijiang fault into Dianzhong) and the contrast across Longmenshan between moderately low wave speeds in Songpan and high wave speeds beneath Sichuan Basin. Weak and spatially

¹State Key Laboratory of Earthquake Dynamics, Institute of Geology, CEA, Beijing 100029, China, ²Department of Earth, Atmospheric and Planetary Sciences, MIT, Cambridge, Massachusetts 02139, USA, ³Laboratory of Seismology and Physics of Earth's Interior, School of Earth and Space Sciences, USTC, Hefei, Anhui 230026, China. *e-mail: qyliu@ies.ac.cn

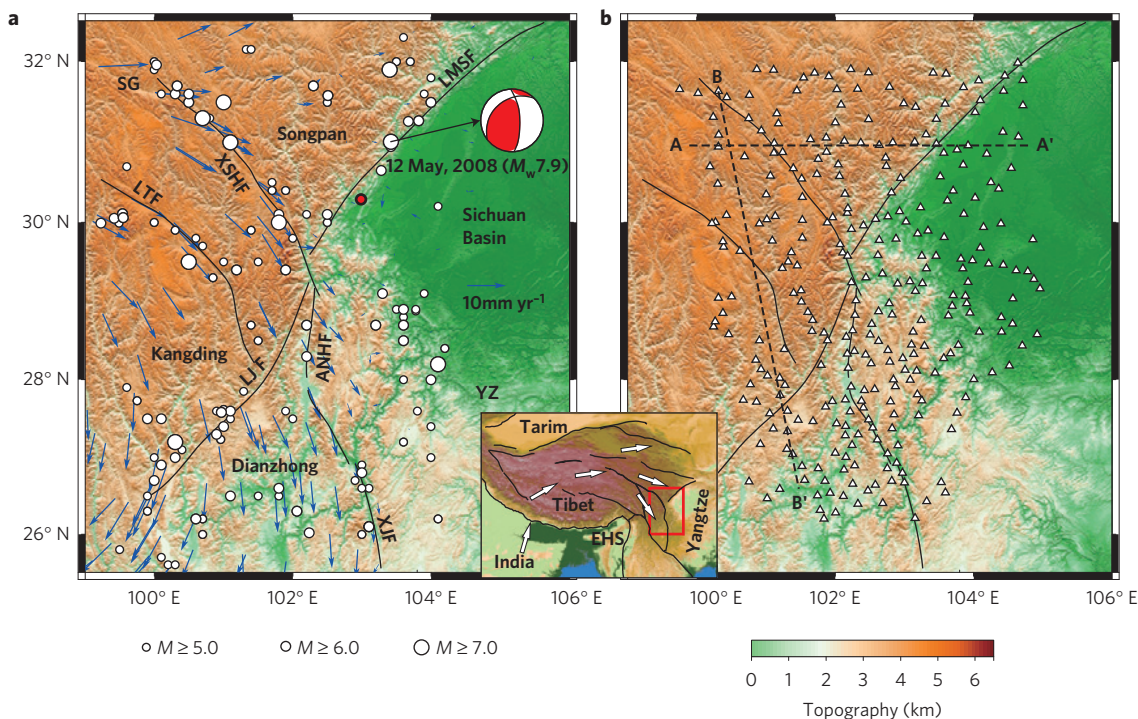


Figure 1 | Maps of western Sichuan. **a**, Geological setting. Black solid lines indicate faults. White circles: epicentres of earthquakes ($M_s > 5.0$) between 1901 and 2010 (source: China Earthquake Network Center). Symbol size scales with magnitude. Red circle: Lushan earthquake ($M_w = 6.6$; 20 April 2013); focal mechanism: 2008 Wenchuan earthquake (source: global CMT catalogue). Blue arrows: (geodetic) crustal motion relative to the Yangtze craton¹. **b**, Location of the (temporary) seismograph array (297 broadband stations; 10–30 km spacing; operational from 2006–2009). Black solid lines and open triangles: faults and stations, respectively. Dashed lines: location of the sections in Fig. 3. Inset: white arrows indicating large scale block motion. Acronyms: EHS, Eastern Himalaya Syntaxis; SG, Songpan–Ganze; YZ, Yangtze; XSHF, Xianshuihe fault; LMSF, Longmenshan fault; LJF, Lijiang–Xiaojinhe fault; ANHF, Anninghe fault; XJF, (Zemuhe–)Xiaojiang fault; LTF, Litang fault.

variable slow anomalies are detected in Yangtze. Between 50 and 80 km depth (Fig. 2d–f) the Longmenshan and Lijiang faults mark a sharp transition between seismically fast (cratonic) mantle to the east and low (deep crustal and uppermost mantle) wave speeds to the west, with subtle differences across the Xianshuihe fault. Figure 2 suggests that Longmenshan and Lijiang are main boundary faults, marking lateral differences between the plateau and craton structure to lower crustal depths.

Vertical sections further illustrate the transition from the relatively simple lithosphere of the Yangtze craton (including Sichuan Basin) to the structural complexity of the Tibetan plateau. The choice of profiles (Fig. 3) was motivated by predictions from the channel flow model^{8,9} (Supplementary Fig. 16): section A–A' crosses the steep drop in elevation from plateau to basin across Longmenshan and section B–B' follows the gentle topographic gradient from the high plateau into Yunnan. We note that the features discussed below are also clear in other cross-sections (Supplementary Figs 12, 13 and 15).

Before discussing structural changes across the main boundary faults, we make the following general observations. First, east of the Longmenshan and Lijiang faults the base of the crust (white line, Fig. 3) is unequivocal given the tomographically inferred radial wave speed variations and evidence for a distinct Moho from receiver functions (Supplementary Figs 4 and 5). Second, west of these faults crust-like wave speeds extend to greater depths and receiver functions are ambiguous and often lack distinct wave conversions (Supplementary Figs 4, 11, 12 and 13). This suggests that there is no sharp Moho and that the crust–mantle transition is gradual (dashed lines), which is common in tectonically active areas. We note that our first-order observations regarding crustal thickness do not depend on the precise nature of the transition. Third,

consistent with previous studies^{21–23}, the increase in crustal thickness from ~40 km in Sichuan Basin (~50 km in Yangtze) to 60–80 km beneath the plateau occurs over a relatively small lateral distance, with evidence for some thickening of the deep crust towards the craton (Supplementary Fig. 15). Fourth, whereas the entire crust beneath southeastern Tibet is (seismically) slower than the global average, zones with anomalously low velocity (LVZs) appear in the Kangding and Songpan units (Supplementary Figs 12, 13 and 15). Fifth, the apparent structural homogeneity of the deep crust west of the boundary faults suggests continuous deformation of the deep crust beneath eastern Tibet.

Sections A–A' and B–B' differ in important aspects, with lateral contrasts across the Longmenshan fault (Fig. 3a) more pronounced than across the Lijiang fault (Fig. 3b). The former coincides with steep topographic relief and the edge of a mid-crustal LVZ—both the middle and lower crust contribute to crustal thickening relative to Sichuan Basin, but the onset of lower crustal thickening is a few tens of kilometres west of the topographic break and surface expression of the Longmenshan fault (Supplementary Fig. 15). The Lijiang fault coincides with a subtle but distinct change in relief (Figs. 1, 4) and with a change in stress orientation inferred from earthquake focal mechanisms (N–S to E–W extension)⁷. Thickening of plateau crust (compared to that of Yangtze craton) seems here confined to the transitional lower part, and the mid-crustal LVZ protrudes across the fault—beyond the area of thick crust—as far east as the Emeishan igneous province²⁰.

Figure 4 summarizes the 3D wave speed variations inferred from the array data and highlight spatial correlations between crustal heterogeneity and surface features. Changes in elevation and in crustal structure and thickness—in particular the extent of deep crustal thickening—suggest that the Longmenshan and Lijiang

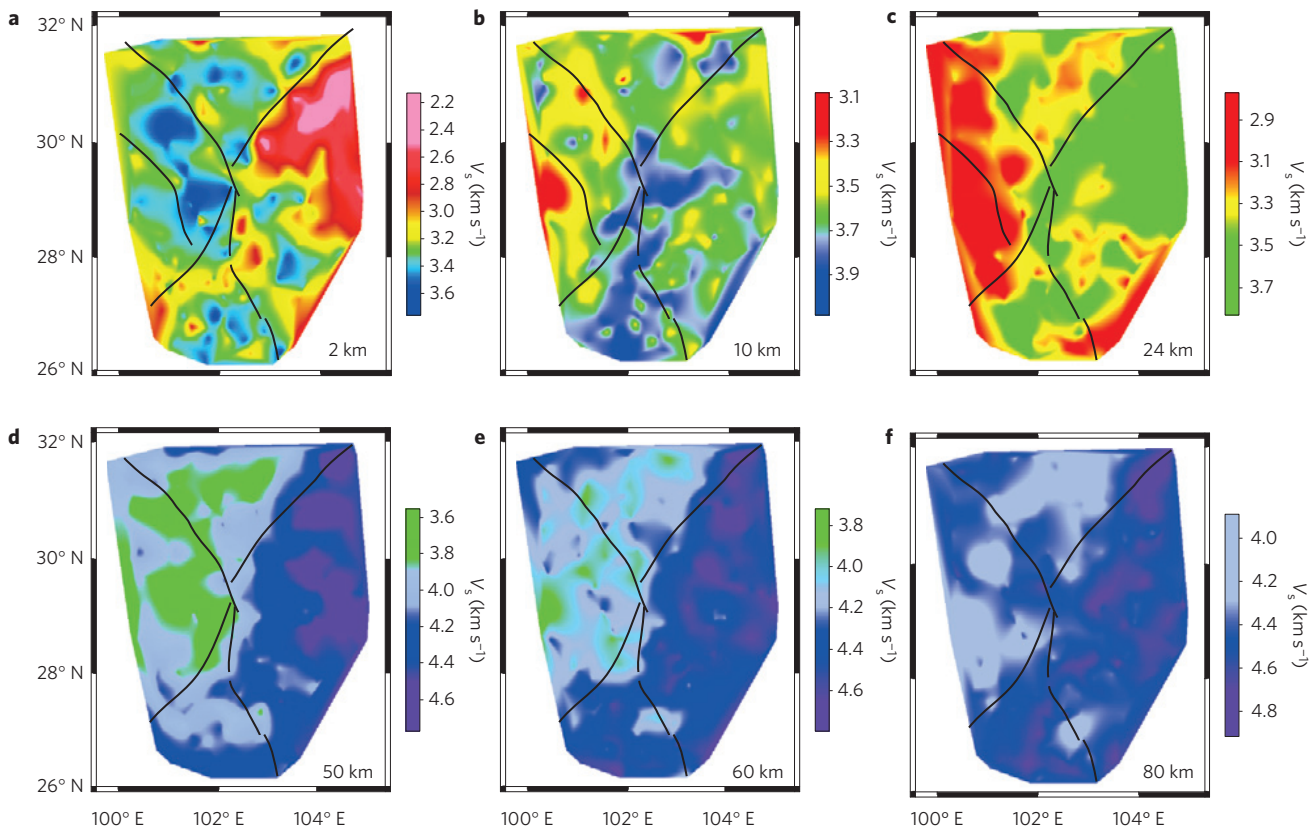


Figure 2 | Map views of wave speed variation in crust and mantle. a–f, Results of the joint inversion of P-receiver functions and (ambient noise) surface wave dispersion measured from the dense seismograph array depicted in Fig. 1b (see Supplementary Information for a description of the method). The depth (below sea level) of each map view is shown in the lower right corner. Black solid lines denote major faults (Fig. 1).

faults mark the main (western) boundary of the Yangtze craton. In the north, at the Longmenshan, this boundary is quite sharp and manifests at all depths. In the south (in Dianzhong), Tibetan crust transgresses (locally) onto the lithospheric root of the craton. The Xianshuihe fault marks the northern edge of a pronounced, laterally continuous LVZ.

The combination of slow shear wave propagation, high Poisson's ratios¹⁴ and differential crustal thickening suggests that the plateau is, overall, mechanically weak compared to the Yangtze craton. Differences exist, however, between the main units comprising the plateau. South of the Xianshuihe fault (in Kangding, at the eastern end of the central Tibetan Qiangtang unit) zones of anomalously low velocities ($< 3.3 \text{ km s}^{-1}$), strong radial anisotropy ($V_{sh} > V_{sv}$; ref. 18), and high electrical conductivity¹³ suggest that the middle crust is weak even compared to the overall crust and that interconnected ductile flow is possible. These weak zones may be related to magmatism in and flow from central Tibet²³, and in the absence of (present-day) obstacles to further eastward motion, detached (by the Xianshuihe fault) from the more stagnant Songpan unit further north, and aided by gravitational driving forces⁷, they facilitate lateral displacement of the brittle upper crust around EHS, as observed geodetically^{1–3}. It is possible that shear heating due to differential motion between upper crust and lithospheric mantle further reduces viscosities, enhancing LVZs and causing a dynamic run-away. Continuation of weak crust onto the Yangtze cratonic keel (Fig. 3b) can explain the gentle topographic slope and accommodate the increase in surface velocities towards Yunnan (in a Tibetan Plateau fixed reference frame)³.

North of the Xianshuihe fault, in the Songpan unit, the array data resolve crustal LVZs that are smaller—both in strength ($3.3 < V_s < 3.5 \text{ km s}^{-1}$) and size—than beneath Kangding, located

at variable depths, and cut off in the east by the Longmenshan fault (Figs 2c and 3a). These LVZs may involve partial melt^{24–26}, but the average crustal viscosity here is probably higher than in Kangding. Obstruction of eastward motion by Sichuan Basin may produce crustal thickening and local strain heating²⁷ but prevent the run-away that may help produce the extensive LVZ further south.

These lateral variations in crustal rheology and boundary conditions ('strong' across Longmenshan, 'weak' across Lijiang fault) help in understanding regional seismicity. Along with surface uplift in Songpan from levelling surveys², our results support the interpretation that the 2008 Wenchuan earthquake ($M = 7.9$; thrust near epicentre, increasing right-lateral slip northeastwards along Longmenshan^{12,28}) resulted from uplift of brittle upper crust²⁹. In contrast, ductile flow beneath Kangding and the weakness of (lateral) boundaries facilitate energy release, limit earthquake magnitude, and localize the transition from normal fault earthquakes with N–S extension (above the LVZ in Kangding) to normal faulting with E–W extension (in Dianzhong)⁷.

The differences between the Songpan (A–A') and Kangding (B–B') transitions as well as the eastward thickening of lower crust towards the craton (Figs 3 and 4) are qualitatively consistent with the notion of channel flow^{8,9} (Supplementary Fig. 16). Our results suggest, however, that such flow is not uniform and that deformation of the eastern Tibetan Plateau is influenced by (mechanical) conditions along the periphery, lateral variations in crustal structure and rheology, and strain partitioning across major (strike-slip) faults. Deformation through the interaction of crustal blocks that are internally deformed, which may (or may not) contain interconnected weak zones, and which are separated by deep-cutting faults, reconciles the canonical endmember models

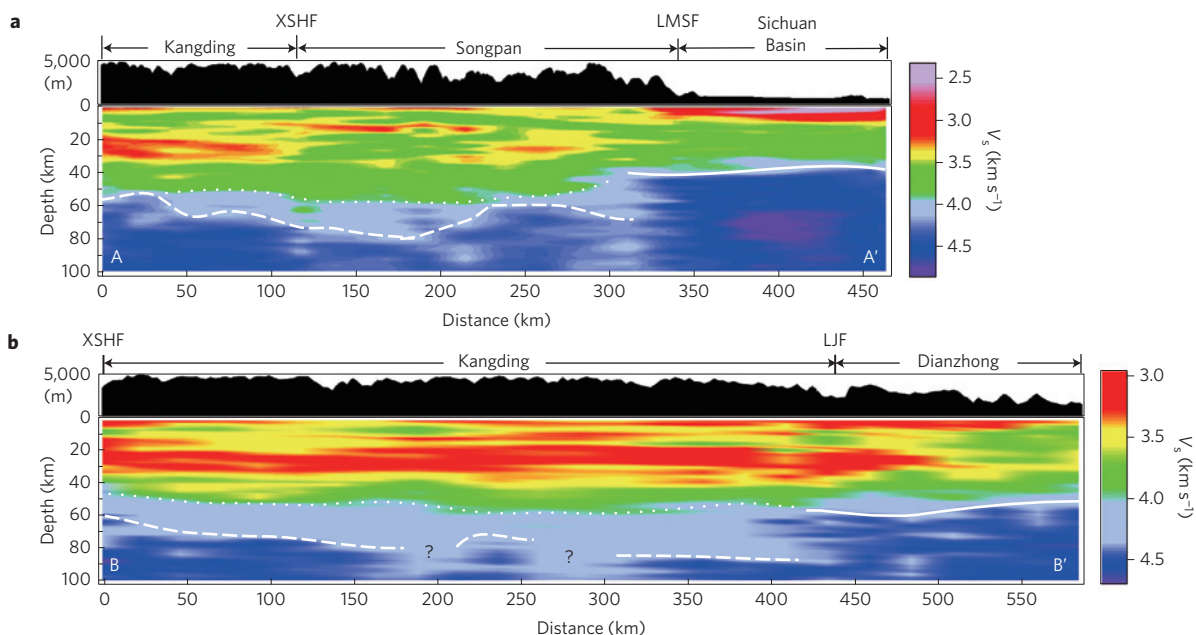


Figure 3 | Vertical sections through the 3D wave speed model. **a**, A–A' crosses the Longmenshan and the epicentre of the 2008 Wenchuan earthquake. **b**, B–B' follows the gentle topographic gradient from the high plateau into Yunnan. Solid white lines: Moho (if receiver functions and surface wave dispersion are both consistent with a sharp crust–mantle boundary). White dotted and dashed lines: top and bottom of transitional crust (if dispersion suggests a gradual wave speed increase and receiver functions lack evidence for a sharp boundary). Sichuan Basin is characterized by high wave speeds in the shallow mantle; eastern Tibetan Plateau is characterized by large but laterally variable crustal thickness, distinct intra-crustal low-velocity zones, and a transitional crust–mantle boundary. Acronyms as in Fig. 1.

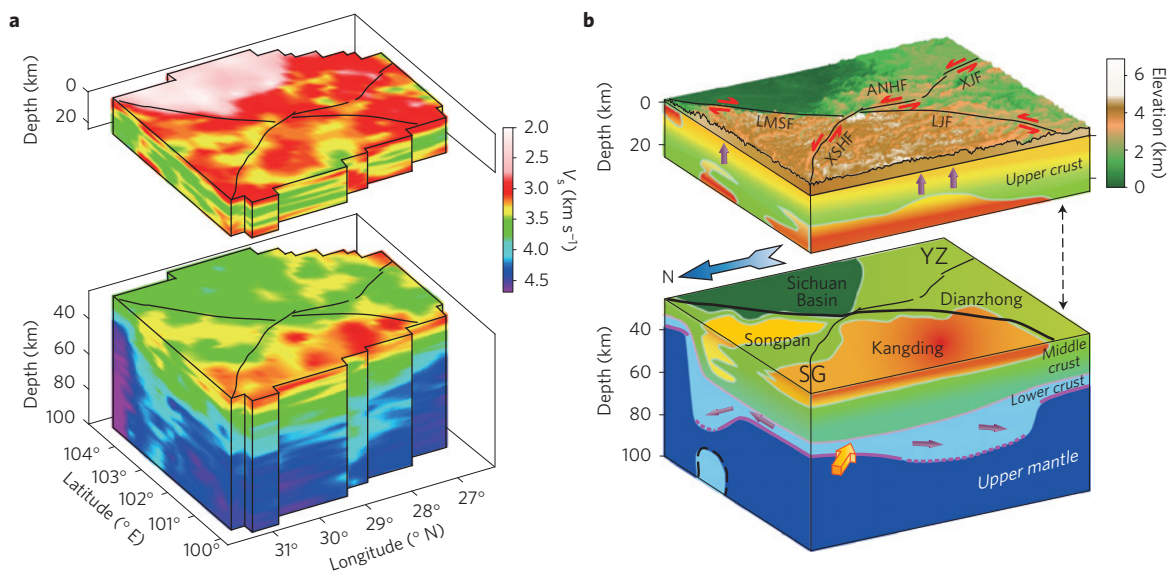


Figure 4 | 3D perspectives of lithospheric shear-wave speed variations in relation to surface topography and major fault systems. **a**, Wave speed from joint inversion. **b**, Cartoon summarizing the main structural and topographic features. Black thin solid lines depict faults. Black thick solid lines depict the eastern border of the Tibetan plateau from this study. Purple solid and dashed lines depict the clear and unclear crust–mantle boundary, respectively. Yellow cubic arrow indicates the general (eastward) direction of the deep crustal flow. Purple arrows indicate the upper crust uplift and the lower crustal deformation in each unit. Acronyms as in Fig. 1.

of deformation through (rigid) block motion along faults^{4,5} or crustal flow^{8,9}.

Methods

On the one hand, receiver functions sense elasticity contrasts but cannot constrain interface depths without knowledge of the absolute wave speed. On the other hand, surface wave dispersion (here extracted from ambient seismic noise¹⁵) is more sensitive to wave speed variations than to interface depths. Joint inversion of receiver functions and surface wave dispersion constrains interface depth

as well as lateral wave speed variations. The method—based on Bayesian theory³⁰—is described in the Supplementary Information. Joint inversion provides better constraints on wave speed variations and interface depths, but crustal thickness estimates can differ from the separate inversion of receiver functions, especially if the crust–mantle boundary is transitional, as is often the case for tectonically active regions such as the region under study.

Received 29 May 2013; accepted 5 March 2014;
published online 30 March 2014; corrected online 2 April 2014

References

- Wang, Y. *et al.* GPS-constrained inversion of present-day slip rates along major faults of the Sichuan–Yunnan region. *China Sci. China Ser. D* **51**, 1267–1283 (2008).
- Zhang, P. Z. *et al.* Continuous deformation of the Tibetan Plateau from global positioning system data. *Geology* **32**, 809–812 (2004).
- Gan, W.-J. *et al.* present-day crustal motion within the Tibetan Plateau inferred from GPS measurements. *J. Geophys. Res.* **112**, B08416 (2007).
- Tapponnier, P. *et al.* Propagating extrusion tectonics in Asia: New insights from simple experiments with plasticine. *Geology* **10**, 611–616 (1982).
- Tapponnier, P. *et al.* Oblique stepwise rise and growth of the Tibet Plateau. *Science* **294**, 1671–1677 (2001).
- Houseman, G. & England, P. Crustal thickening versus lateral expulsion in the Indian–Asian continental collision. *J. Geophys. Res.* **98**, 12233–12249 (1993).
- Copley, A. Kinematics and dynamics of the southeastern margin of the Tibetan Plateau. *Geophys. J. Int.* **174**, 1081–1100 (2008).
- Royden, L. H. *et al.* Surface deformation and lower crustal flow in Eastern Tibet. *Science* **276**, 788–790 (1997).
- Clark, M. K. & Royden, L. H. Topographic ooze: Building the eastern margin of Tibet by lower crustal flow. *Geology* **28**, 703–706 (2000).
- Hubbard, J. & Shaw, J. H. Uplift of the Longmen Shan and Tibetan plateau, and the 2008 Wenchuan ($M = 7.9$) earthquake. *Nature* **458**, 194–197 (2009).
- Wang, E. *et al.* Two-phase growth of high topography in eastern Tibet during the Cenozoic. *Nature Geosci.* **5**, 640–645 (2012).
- Zhang, P. Z., Wen, X. Z., Shen, Z. K. & Chen, J. H. Oblique, high-angle, listric-reverse faulting and associated development of strain: The Wenchuan earthquake of May 12, 2008, Sichuan, China. *Annu. Rev. Earth Planet. Sci.* **38**, 351–380 (2010).
- Bai, D. *et al.* Crustal deformation of the eastern Tibetan plateau revealed by magnetotelluric imaging. *Nature Geosci.* **3**, 358–362 (2010).
- Xu, L., Rondenay, S. & Van der Hilst, R. D. Structure of the crust beneath the Southeastern Tibetan Plateau from teleseismic receiver functions. *Phys. Earth Planet. Int.* **165**, 176–193 (2007).
- Yao, H., Beghein, C. & van der Hilst, R. D. Surface wave array tomography in SE Tibet from ambient seismic noise and two-station analysis–II. Crustal and upper-mantle structure. *Geophys. J. Int.* **173**, 205–219 (2008).
- Li, H., Su, W., Wang, C. Y. & Huang, Z. Ambient noise Rayleigh wave tomography in western Sichuan and eastern Tibet. *Earth Planet. Sci. Lett.* **282**, 201–211 (2009).
- Yao, H., van der Hilst, R. D. & Montagner, J. P. Heterogeneity and anisotropy of the lithosphere of SE Tibet from surface wave array tomography. *J. Geophys. Res.* **115**, B12307 (2010).
- Huang, H., Yao, H. & van der Hilst, R. D. Radial anisotropy in the crust of SE Tibet and SW China from ambient noise interferometry. *Geophys. Res. Lett.* **37**, L21310 (2010).
- Wang, C. Y., Han, W. B., Wu, J. P., Lou, H. & Chan, W. W. Crustal structure beneath the eastern margin of the Tibetan Plateau and its tectonic implications. *J. Geophys. Res.* **112**, B07307 (2007).
- He, B., Xu, Y. G., Chung, S. L., Xiao, L. & Wang, Y. Sedimentary evidence for a rapid, kilometer-scale crustal doming prior to the eruption of the Emeishan flood basalts. *Earth Planet. Sci. Lett.* **213**, 391–405 (2003).
- Zhang, Z. *et al.* Seismic signature of the collision between the east Tibetan escape flow and the Sichuan Basin. *Earth Planet. Sci. Lett.* **292**, 254–264 (2010).
- Robert, A. *et al.* Crustal structures in the area of the 2008 Sichuan earthquake from seismologic and gravimetric data. *Tectonophysics* **491**, 205–210 (2010).
- Wang, Y., Mooney, W. D., Yuan, X. & Okaya, N. Crustal Structure of the Northeastern Tibetan Plateau from the Southern Tarim Basin to the Sichuan Basin, China. *Tectonophysics* **584**, 191–208 (2013).
- Beaumont, C., Jamleson, R. A., Nguyen, M. H. & Lee, B. Himalayan tectonics explained by extrusion of a low-viscosity crustal channel coupled to focused surface denudation. *Nature* **414**, 738–742 (2001).
- Nelson, K. D. *et al.* Partially molten middle crust beneath southern Tibet; synthesis of Project INDEPTH results. *Science* **274**, 1684–1688 (1996).
- Kind, R. *et al.* Evidence from earthquake data for a partially molten crustal layer in south Tibet. *Science* **274**, 1692–1694 (1996).
- Leloup, P. H. *et al.* Shear heating in continental strike-slip shear zones: model and field examples. *Geophys. J. Int.* **136**, 19–40 (1999).
- Xu, X. W. *et al.* Coseismic reverse- and oblique-slip surface faulting generated by the 2008 Mw 7.9 Wenchuan earthquake, China. *Geology* **37**, 515–518 (2009).
- Burchfiel, B. C. *et al.* A geological and geophysical context for the Wenchuan earthquake of 12 May 2008, Sichuan, People's Republic of China. *GSA Today* **18**, 4–11 (2008).
- Liu, Q. Y. *et al.* Joint inversion of receiver function and ambient noise based on Bayesian theory. *Chin. J. Geophys.* **53**, 240–251 (2010).

Acknowledgements

The authors benefited from discussions with P. Z. Zhang, L. H. Royden, R. Kind, P. Tapponnier, M. Deves and Y. Z. Wang. This study was granted in part by National Key Basic Research Program (973), Ministry of Science and Technology of China (2004CB418402), State Key Laboratory of Earthquake Dynamics (LED2008B05), Basic Scientific Funding of Institute of Geology, China Earthquake Administration (IGCEA1009), and US-NSF grants EAR0910618 and EAR0003571.

Author contributions

Q.Y.L. and R.D.v.d.H. wrote the paper. All authors discussed the interpretations and commented on the manuscript. Y.L., H.J.Y. and H.H. conducted ambient noise data analyses. J.H.C., B.G., S.H.Q., J.W. and S.C.L. conducted field work and teleseismic data analyses.

Additional information

Supplementary information is available in the online version of the paper. Reprints and permissions information is available online at www.nature.com/reprints. Correspondence and requests for materials should be addressed to Q.Y.L.

Competing financial interests

The authors declare no competing financial interests.

Eastward expansion of the Tibetan Plateau by crustal flow and strain partitioning across faults

Qi Yuan Liu, Robert D. van der Hilst, Yu Li, Hua Jian Yao, Jiu Hui Chen, Biao Guo, Shao Hua Qi, JunWang, Hui Huang and Shun Cheng Li

Nature Geosci. <http://dx.doi.org/10.1038/ngeo2130> (2014); published online 30 March 2014; corrected online 2 April 2014

In the version of this Letter originally published online, the author Jiu Hui Chen was affiliated with the incorrect institution. The correct affiliation is the State Key Laboratory of Earthquake Dynamics, Institute of Geology, CEA, Beijing 100029, China. This has been corrected in all versions of the Letter.